Fusion Engineering and Design 215 (2025) 114950

Contents lists available at ScienceDirect

Fusion Engineering and Design

journal homepage: www.elsevier.com/locate/fusengdes

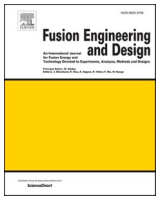

# Temperature dependence of sputtering yields of steels with various W content for plasma facing applications

S. Möller [a,*], M. Reinhart [b], B. Kuhn [c], A. Kreter [b]

[a] Forschungszentrum Jülich GmbH, Institute of Energy Materials and Devices, Materials Synthesis and Processing (IMD-2), 52425 Jülich, Germany
[b] Forschungszentrum Jülich GmbH, Institute of Fusion Energy and Nuclear Waste Management – Plasma Physics, 52425 Jülich, Germany
[c] Deggendorf Institute of Technology, Dieter-Görlitz-Platz 1, 94469 Deggendorf, Germany

ARTICLE INFO

*Keywords:*
Plasma-facing components
Material analysis
Surface analysis
Plasma surface interactions
Steel

ABSTRACT

Materials are a key issue in any nuclear fusion reactor. For plasma-facing materials irradiation and sputtering limit their lifetime in a fusion power reactor. Steels allow for lower costs, reduced activation, and proven long irradiation lifetimes compared to tungsten at the expense of a lower sputtering lifetime.

Several studies investigated the connected effects showing W-fuzz like surface morphology and a W enrichment through preferential sputtering, opening up a potentially significant increase of this sputtering lifetime of steels.

The role of the W content in the steel is an open question. The presented exposure of 3 steels with W content from 0.5 to 2 at. % in deuterium plasma at 693–843 K sample temperature aims at resolving this. The experiments combine in-situ infrared imaging and passive spectroscopy with ex-situ ion-beam analysis.

At the given conditions, a flux density independent exponential W enrichment within 70 s time-constant followed by a 1400 s time-constant nano-structure formation is observed. The overall effect is a reduction of the Fe sputtering yield by a factor 4.4, 3.0, and 2.5 for 2 %, 1.1 %, 0.5 % W steels, respectively. This factor reduces slightly with temperature by up to 20 % towards higher temperatures.

## 1. Introduction

Materials are a key component in any technological development and product. Steels are particularly interesting for fusion as they are the only experimentally tested material known to survive neutron irradiation levels of 200 DPA [1, p. 200], equivalent to ~20 years of fusion reactor operation. While this lifetime is crucial for a structural material, also for plasma-facing materials (PFMs) a long lifetime is desirable. PFM lifetimes are further limited by ion-induced sputtering, but numerous factors influence the sputtering yield. The surface morphology and composition can change the sputtering yields by orders of magnitude. So far, W is considered as the prime candidate PFM due to its long sputtering related lifetime, but its irradiation damage related lifetime is still an open question. Optimising a steel towards a longer sputtering related lifetime en-par with its high irradiation related lifetime would provide fusion reactors with an ideal material.

The physics of plasma surface interaction of steels is significantly more complex compared to elementally pure materials such as W. In particular, the self-organised growth of nano-structures under ion impact and elevated surface temperatures is an effect under active investigation [2–5]. Several studies investigated this effect using hyperspectral imaging [6], passive spectroscopy, active spectroscopy, catchers, and simulations [2–4,7,8]. The nano-structure formation potentially has a strong positive impact on the overall fusion power reactor design, since it can significantly reduce the sputtering yield, leading to reduced armour thicknesses, increased T-breeding, and reduced maintenance costs. At the same time the effect is not completely understood and possibly only a small window in ion flux, ion impact energy, and surface temperature exists where the sputtering related loss of nano-structure thickness equals the growth rate of the nano-structure to enable the formation of a relevant nano-structure thickness.

In [6] it was shown that the sputtering yield of a nano-structured W and Mo surfaces depends on the thickness of the nano-structure (or the received ion fluence), decreasing up to a saturation value of 600–1000 nm by about 60 %. Similar results with higher suppression factors of up to 10 are found in [9]. Interestingly, this thickness range corresponds to the dynamic range limit of infrared (IR) emissivity measurements [10], suggesting a connection between light and particle interaction with the

* Corresponding author.
*E-mail address:* s.moeller@fz-juelich.de (S. Möller).

https://doi.org/10.1016/j.fusengdes.2025.114950
Received 2 December 2024; Received in revised form 13 February 2025; Accepted 7 March 2025
Available online 13 March 2025

surface in the suggested mean-free path concept [6]. Possibly the literature observations on the impact of fuzz grown on W and Mo surfaces generalises to the nano-structures developing on steels. This would improve the general understanding of the mechanisms and ease the integration of the effect into the technical design of functional components in fusion reactors.

Additionally, the enrichment of heavy elements through preferential sputtering [11] influences the effective sputtering yield. The preferential sputtering is most relevant, if the ion impact energy lies above the lighter elements sputtering threshold and below the heavier elements threshold. For D ion impact on steels this range is between ~50 eV (Fe threshold) and ~220 eV (W threshold). Theoretically, W should enrich at the surface to 100 % concentration, independent of its bulk concentration. Unfortunately, observations show a limitation of the heavy element enrichment, probably due to diffusion of Fe and Cr from the bulk. In experiments it can be expected that heavier impurities such as O, with ~30 eV (Fe) and ~60 eV (W) sputtering thresholds, influence the process, depending on the purity of the experimental setup. Therefore, deviations of the results between different experimental setups and theoretical calculations can be expected. Furthermore the parameter space in terms of flux density, fluence, temperature, W bulk concentration, ion impact energy and species is large and not fully explored.

The question investigated in this work is how the heavy element content (mostly W) influences this balance at different temperatures. Can high W steels such as HiperFer (2 at. % W) beat the established fusion steel Eurofer97 (Eu97) with its relatively low ~0.5 at. % W in terms of sputtering lifetime?

## 2. Methods

The samples are 100×80 mm² bulk steel plates made from Eu97 (0.5 % W), Crofer22H (1.1 % W), and HiperFer-Ta (2 % W+Ta), respectively. They were exposed at the linear plasma generator PSI-2 [12] to a maximum ion flux of $3*10^{21}$ D/m²s for about 8h, resulting in an ion fluence of $8*10^{25}$ D/m². PSI-2 features a hollow flux profile with a maximum flux density in a ring of about 25 mm radius. The impurity fraction in PSI-2 is about $10^{-3}$ of the ion flux, mostly due to N and O ions.

The plasma heats the samples to a minimum temperature of 693 K (420 °C). From there on 50 K steps to 743 K, 793 K, and 843 K are made by applying additional resistive heating to the target. The temperature is kept for at least 600 s at each step and then changed to the next step. The temperature is regulated to be within ±5 K of the given value. The nano-structure build-up is derived from the IR emissivity at 5 μm wavelength according to the reference hole approach presented in [10] with a 1 s time resolution. These reference holes are black body emitters with emissivity=1, which enables determining the local emissivity close to the hole through the ratio of the IR intensities of the surface location to the hole. In parallel, a 2D imaging spectrometer, with its line of sight perpendicular to the plasma column, was used to observe Fe and Cr lines in front of the sample with a 60 s time-resolution. The radial profile of these emission lines was calculated by applying an inverse Abel transformation to the line-integrated measurements.

After exposure the samples are removed and transferred to the ion-beam analysis (IBA) mapping using Rutherford-backscattering spectrometry with 1.43 MeV $^4$He ions to investigate the changes of the surface composition using the setup described in [13]. The analysis investigates Fe, Cr, and W content. W in this case sums up all heavy elements, in particular Ta which is present in Hiperfer-Ta.

In order to investigate the theoretical behaviour more realistically and avoid the obvious result (100 % yield reduction due to 100 % tungsten enrichment), a fraction of $10^{-3}$ of the impacting ion flux is assumed as O+. This concentration is typical for PSI-2 and derived from the ratio of background to operating pressure. SRIM2013 calculations using the surface sputtering mode with displacement thresholds of 38 eV (W) and 17 eV (Fe) are assumed in a mixed Fe-W material.

## 3. Results

Fig. 1a shows a photography of the analysed sample. The sample is strongly affected by the plasma exposure visible through a darkening of the formerly polished steel surfaces. The darkening also resembles the ring shaped PSI-2 plasma visible as a maximum in darkening. A recrystallization occurred during the high-temperature exposure of the sample. Fig. 1b show the corresponding Langmuir probe analysis of the plasma parameters. The parallel flux resembles the optical impression of a flux peak of about 10 mm width.

Fig. 2 shows the upper right quadrant of the Hiperfer sample in the IBA analysis. The data in Fig. 2a display the layer thickness of the enriched surface layer, which reproduces the ring structure of the plasma flux profile shown in Fig. 1b. Fig. 2a shows the W enrichment in this surface layer. The enrichment does not match the ring structure of the plasma flux profile, but rather the plasma potential. The W enrichment reduces radially from the plasma centre with a step at the peak flux ring where also the plasma potential has a step. The radial profile fits well to an exponential decay, but the points' scatter is significant. The enrichment percentage scales with the initial W content with W+Ta enrichments of 37 % (HiperFer-Ta), 31 % (Crofer22H), and 27 % (Eu97) in sample centre.

Fig. 3 shows the evolution of the emissivity of the HiperFer-Ta sample over the course of the plasma exposure. This data is analysed using individual linear fits to each section of constant temperature. The resulting linear growth rate of the emissivity (~layer thickness) at fixed temperature demonstrates a connection between sputtering yield and nano-structure layer thickness due to the exponential decrease of the sputtering yields shown in Fig. 4. A thin surface layer does not protect the full surface as the increasing IR emissivity indicates. Assuming that the possibility of IR light reflection equals the possibility of sputtered particle ejection, the IR emissivity would be a direct number for the nano-structure sputtering suppression efficiency. Emissivity and nano-structure thickness are connected with an exponential asymptotic behaviour towards emissivity=1 [10]. The average growth rate of the emissivity averaged over all temperatures and flux densities is $3.7*10^{-5}$/s (Eu97), $1.7*10^{-5}$/s (Crofer), and $1.8*10^{-5}$/s (HiperFer-Ta), respectively. A clear influence of the temperature, flux density, or emissivity on growth rate is not observed, but the amount of data points is low when divided into these dimensions.

While the emissivity increases over time, the sputtering yield of the lighter elements of the steels (Fe and Cr) jumps up with every temperature step as demonstrated in Fig. 4. We can see an exponential decrease of the sputtering yield, similar to the mathematically formulation in [3]. The decay is fitted best with a dual (first step) or single (consequent steps) exponential decay with offset ($R^2$=0.990 to 0.997). The decay time constants are in the order of 70 s and 1400–2900 s in the different flux positions. In the flux peak, this corresponds to a fluence of $1.7*10^{23}$ and $3.5*10^{24}$, respectively. Multiplied with the Fe sputtering yield of $2*10^{-2}$ we obtain a removal of $3.4*10^{21}$ sputtered atoms, which is identical with the enriched layer thickness, see Fig. 2a. The relation holds approximately for all 6 positions, since the enriched layer thickness shown in Fig. 2a scales proportionally with the flux density.

The offset of the exponential fit represents the line emission intensity expected for infinite fluence. Interestingly, the fits mostly lead to the same offset value, equivalent to a negligible influence of the temperature on the final sputtering yield. Fig. 4b demonstrates this for the Cr line in the HiperFer experiment, where a maximum sputtering of 1220 units is observed. The minimum offset is 186 units which increase to a maximum of 236 units for 793 K.

Passive spectroscopy in the given wavelength range does not allow for an absolute quantification of the sputtering yield, since the flux of released atoms is not fully covered and quantified by our approach. Only the relative evolution of the sputtering yield can be determined from spectroscopy. The experiment starts with a polished surface of bulk composition, therefore the initial spectroscopy signal is interpreted to

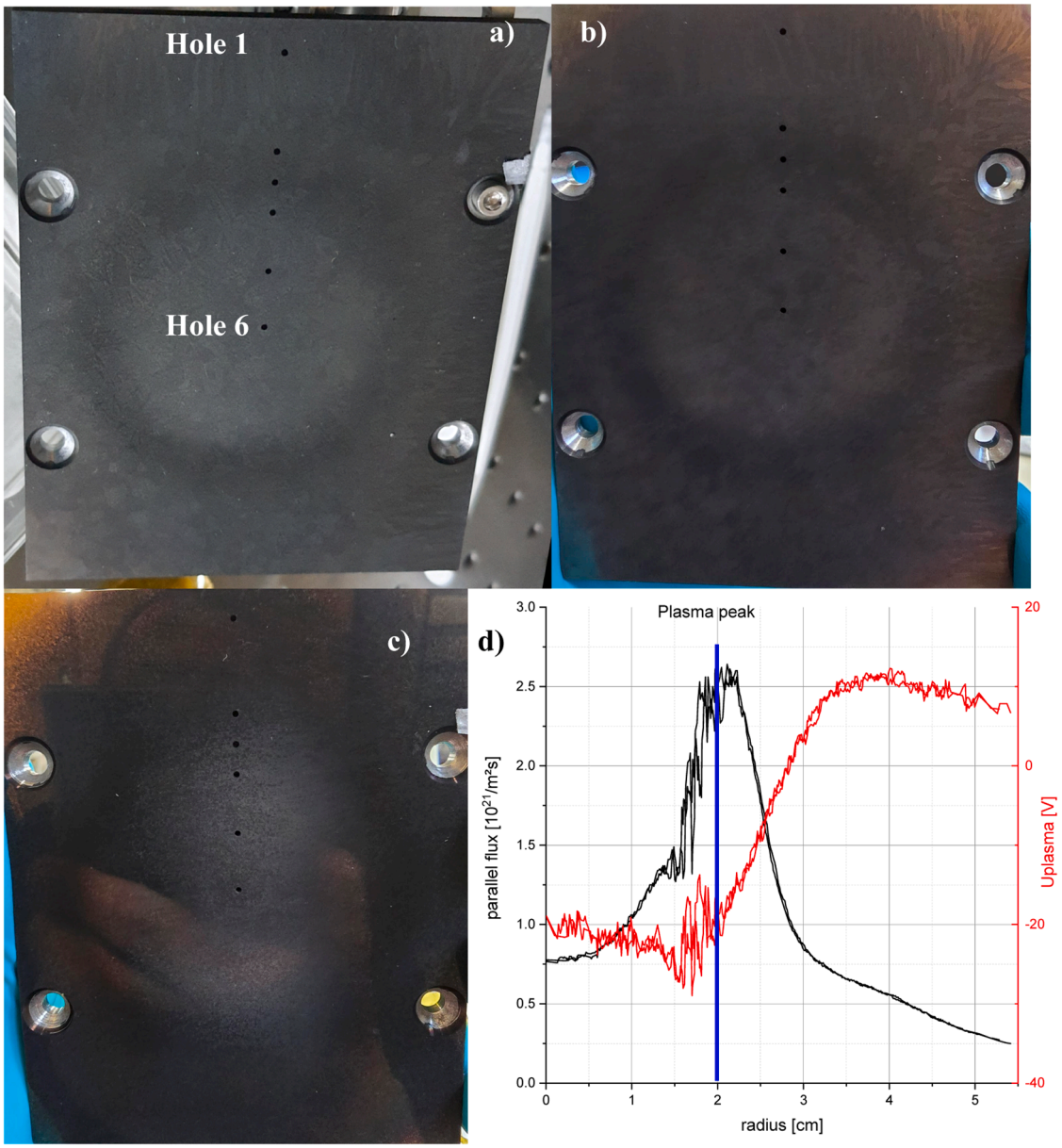


**Fig. 1.** Post exposure photography of the Eu97 a), the HiperFer-Ta b), and the Crofer22H c) samples (80×100 mm²). The six 1 mm diameter IR reference holes and the darker ring of peak plasma flux, related to the PSI-2 hollow cylinder cathode, are clearly visible. IBA investigates the upper left quadrant of the sample surface. d) Corresponding plasma flux profile and plasma potential with the sample centre at radius=0. The images support the assumption of a radial symmetry. The other sample have identical optical impression after exposure.

represent the theoretical sputtering yield obtained under perpendicular incidence on a flat surface of bulk composition. The reduction factor for the sputtering yield is calculated by dividing this initial maximum intensity by the minimum intensity (=minimum offset described above) at a given temperature.

From this we calculate reduction factors between 5.1 at 793 K and 6.4 at 693 K for Cr in HiperFer-Ta. These values are consistent along the sample radius. The observed maximum reduction factors for Fe are somewhat lower with 4.4 (HiperFer-Ta), 3.0 (Crofer), and 2.5 (Eu97), which is in line with the slightly lower sputtering yield of Fe compared to Cr. The high slope in the beginning of the sputtering process, where the reference value of the reduction factor is taken from, and the 60 s time resolution result in highly asymmetric uncertainties of +25 %, -5 % in the reduction factors.

The SRIM calculations using 150 eV O ion impact show equal sputtering yields of Fe and W at an enrichment of 82 % W with a yield of $5*10^{-2}$ per O ion. The 150 eV D ion related Fe sputtering yield for an 82 % W material is $2.5*10^{-4}$ per D ion, significantly below the literature value of $2*10^{-2}$. Taking into account the $10^{-3}$ flux fraction of O ions, sputtering is still dominated by D ions, even at this high W enrichment. At the observed 37 % W enrichment, 5.9 times more Fe than W atoms are sputtered with yields of 0.26 (Fe) and 0.044 (W) per O ion.

## 4. Conclusions

The comparison of the sputtering of 3 steels with W concentrations of 0.5, 1.1, and 2 at. % using in-situ and ex-situ analysis successfully revealed relevant differences between the materials. The samples are exposed to temperatures 693–843 K (420–570 °C) and flux densities (0.5–2.5 $10^{21}$ D/m²s) representative for the first-wall of a fusion power reactor. The steel samples are exposed at 150 eV ion impact energy, a value above the Fe and Cr sputtering threshold, but below the W

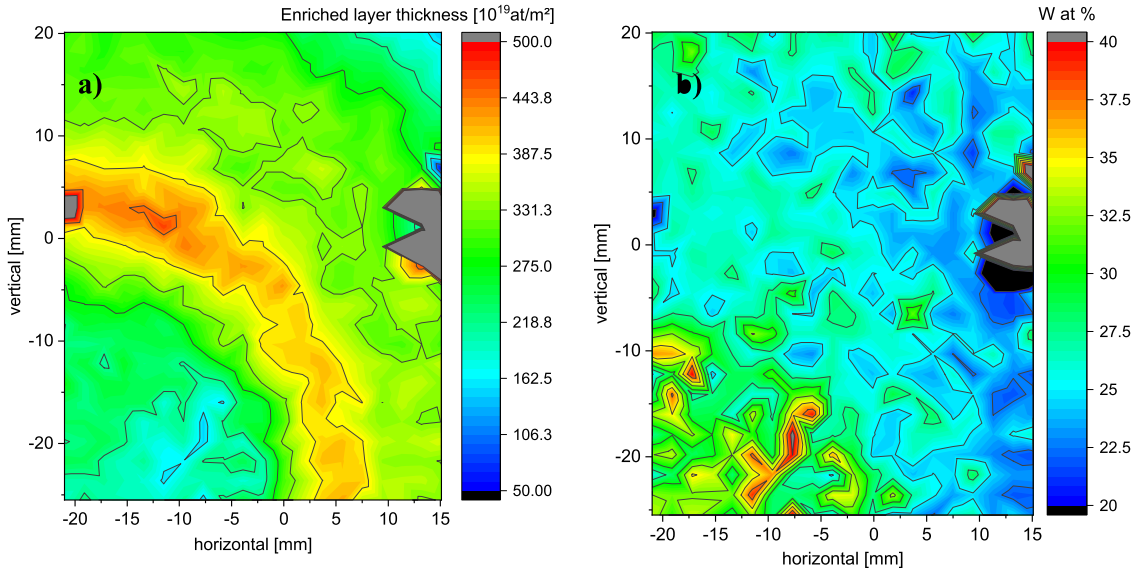


**Fig. 2.** IBA mapping of the upper right quadrant of the Hiperfer-Ta sample. The orientation equals Fig. 1a. The blue or grey part on the right is the mounting screw hole and the red part on the top corresponds to one of the reference holes accidentally being in the analysis grid. In the lower left, the maximum flux region is visible through an increased enriched layer thickness content in a circular shape. The W enrichment on the other hand exponentially increases from ~25 at. % to ~35 at. % from the farthest point towards the plasma centre.

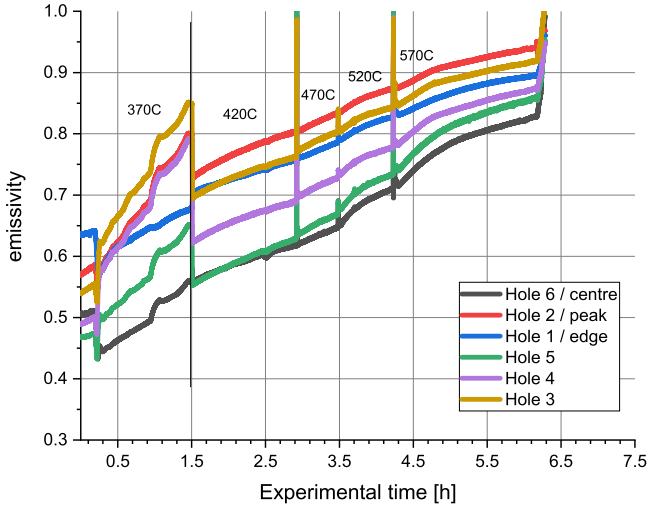


**Fig. 3.** Plot of the HiperFer-Ta emissivity evolution at the 6 observation positions close to the holes and the corresponding temperature steps. The emissivity at the maximum plasma flux in the region of the points 2 and 3 grows fastest.

sputtering threshold. The influence of the bulk W concentration on the W enrichment of the surface layer and the formation of nano-structures is investigated through a combined in-situ and ex-situ analysis approach.

We observe a factor of up to 4.4 in Fe sputtering yield reduction with more W content resulting in higher reduction factors after the settling time. The values for Eurofer agree roughly with literature findings on the sputtering yield reduction factor and the heavy metal enrichment [4]. Steels with significantly higher W content (here Crofer and HiperFer) have not been studied to our knowledge. Studies at higher fluences [14] suggest a continuation of the increase of this factor at even higher fluxes, but the extrapolation of the evolution of the reduction factor observed here opposes this assumption. Nevertheless, at higher fluences additional effects could lead to deviations from our extrapolation. The presented SRIM calculations suggest at higher fluences, with correspondingly thicker nano-structures suppressing the diffusion of Fe and Cr towards to plasma contact layer, the W enrichment should further increase resulting in even higher reduction factors.

The formation of nanostructures on steel shows similarities to the W-fuzz formation, although it is triggered by hydrogen not He ion impact. The structures have a similar appearance when comparing the images from our last work [8] with W-fuzz modelling [15] and W-fuzz observations [6]. W-fuzz growth modelling shows a suppression factor of 6–10, a value comparable to the reduction factors found here. Lastly, we see a similar exponential decay of the yield with exposure fluence as for W-fuzz [9]. From this, we expect the underlying physics of W-fuzz and steel nanostructure formation to be identical.

The decay of the sputtered atom signal, the ion-beam surface analysis, and the sputtering calculations clarify the details of both effects leading to a reduction in sputtering yield. The enrichment process finishes on the time-scale of ~70 s at the given fluxes. This time component diminishes in subsequent temperature steps, showing that the W enrichment fraction is independent of temperature but only the inventory of lighter elements (mainly Fe and Cr) to be removed grows with temperature. This is in agreement with earlier studies on the Fe sputtering yield in steel, showing mostly constant yields in the temperature region investigated here [16].

On the time-scale of 25–50 minutes, the surface nano-structure develops to a relevant thickness. In this phase the reduction factor shifts from W enrichment dominated to a mix of nano-structure and enrichment influences. In the initial phase, the sputtering reduction effect grows with an exponential saturation with the nano-structure thickness. This can be derived from the linear growth rate of the nano-structure seen in the IR data and the exponential decay of the sputtered atom spectroscopy signal. The observed match of the suppression factor ratio of Fe and Cr to their sputtering yield ratio supports the assumption of a pure refractory metal (W+Ta) enrichment and a depletion of the main elements (Fe and Cr). Once a certain nano-structure thickness in the order of ~1 μm is reached, the sputtering reduction saturates. Higher temperatures drive more Fe and Cr towards the surface, but without significant effect on the sputtering yield reduction on longer time-scales beyond the diffusion time-scale. The exponential or square-root flux density dependencies of the nanostructure growth rate seen in earlier works on W fuzz are not reproduced, but a different behaviour of steels and pure W is not unexpected.

The W enrichment is seen to be higher in the plasma centre, where the ion impact energy is ~25 eV lower due to the shifted plasma

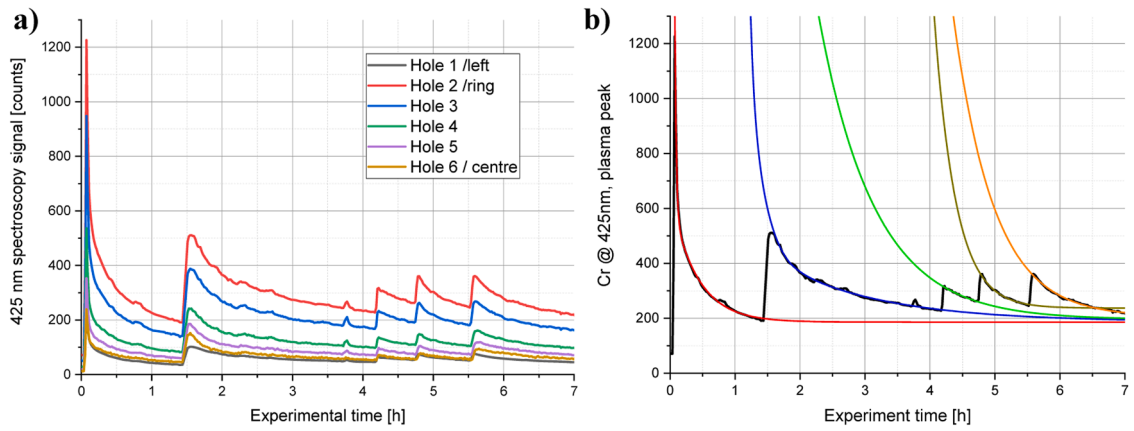


**Fig. 4.** Exemplary plots of the signal evolution in the passive spectroscopy evaluated on the HiperFer-Ta sample. a) shows the 425 nm line associated with the sputtering of Cr at the 6 different radii. b) shows the Cr signal at the plasma peak (hole 2) fitted with individual exponential decays according to A+B×exp(-x/C) for every temperature step. Every signal jump corresponds to a sample temperature step of ~50 K followed by a constant temperature phase.

potential. This demonstrates a direct connection of the maximum W enrichment with the ratio of physical sputtering yields of W and Fe. Direct W or Fe re-deposition is very low in PSI-2 and the differences in the sputtering yield reduction factor are within 5 % along the plasma radius. Compared to a reduction of a factor 4.4, the up to 37 % reduction (factor = 1.6) expected ideally from the W enrichment is small. This both indicates the effect of the nano-structure dominates over the W enrichment in reducing the sputtering yield.

The W enrichment reaches only 37 % in the highest case with a linear dependence on the steel bulk W concentration. This dependence suggests that diffusive processes are important for the maximum W enrichment. Interestingly the nano-structure growth rate and the sputtering suppression factor do not show a clear temperature dependence, which should be significant in a diffusion process. The underlying diffusion process has to be defined by the steel itself, where both W and Fe depend on the same diffusion activation energy defined by the steel composition and structure.

A higher W content in the steel is demonstrated to increase its sputtering resistance, even though the investigated fractions are $\leq$2 %, a fraction too small for an impact by itself. This suggests adding even more W to the steels to boost the effect, but at some point, the benefits of steel diminish. The authors believe, in particular for welding and processing the 2 % W in HiperFer-Ta represent the absolute maximum. At higher ion impact energies the observed effects will change, but in the case of finite tungsten sputtering yields, steels and tungsten could reach similar sputtering yields. This requires further investigations, but the given results indicate steels can be an attractive option for future fusion power reactor plasma-facing materials.

## CRediT authorship contribution statement

**S. Möller:** Writing – review & editing, Writing – original draft, Visualization, Validation, Software, Project administration, Methodology, Investigation, Formal analysis, Data curation, Conceptualization. **M. Reinhart:** Writing – review & editing, Visualization, Investigation, Formal analysis, Data curation, Conceptualization. **B. Kuhn:** Resources, Conceptualization. **A. Kreter:** Supervision, Resources, Funding acquisition.

## Declaration of competing interest

The authors declare that they have no known competing financial interests or personal relationships that could have appeared to influence the work reported in this paper.

## Data availability

All data generated or analysed during this study are available from the authors upon reasonable request.

## References

[1] D.S. Gelles, Microstructural examination of commercial ferritic alloys at 200 dpa, J. Nucl. Mater. 233–237 (1996) 293–298, https://doi.org/10.1016/S0022-3115(96)00222-X.
[2] M. Balden, S. Elgeti, M. Zibrov, K. Bystrov, T.W. Morgan, Effect of the surface temperature on surface morphology, deuterium retention and erosion of EUROFER steel exposed to low-energy, high-flux deuterium plasma, Nucl. Mater. Energy 12 (2017) 289–296, https://doi.org/10.1016/j.nme.2017.01.001.
[3] K. Sugiyama, et al., Erosion of EUROFER steel by mass-selected deuterium ion bombardment, Nucl. Mater. Energy 16 (2018) 114–122, https://doi.org/10.1016/j.nme.2018.05.021.
[4] R. Arredondo, et al., Impact of surface enrichment and morphology on sputtering of EUROFER by deuterium, Nucl. Mater. Energy 23 (2020) 100749, https://doi.org/10.1016/j.nme.2020.100749.
[5] L. Qiao, H. Zhang, C. Xu, E. Fu, P. Wang, Erosion and fuel retentions of various reduced-activation ferritic martensitic steel grades exposed to deuterium plasma, Fusion Eng. Des. 143 (2019) 188–195, https://doi.org/10.1016/j.fusengdes.2019.03.200.
[6] 'Hyperspectral Imaging and TRI3DYN Simulation Study of Physical Sputtering from a Fuzzy Surface - ScienceDirect'. Accessed: Jan. 02, 2024. [Online]. Available: https://www.sciencedirect.com/science/article/pii/S235217912300217X?via%3Dihub.
[7] T. Sarmah, et al., Exposure of Indian RAFM under variation of He$\mathplus$ flux and target temperature in the CIMPLE-PSI linear device, Nucl. Fusion 60 (10) (2020) 106026, https://doi.org/10.1088/1741-4326/abae46.
[8] M. Reinhart, S. Möller, A. Kreter, M. Rasinski, B. Kuhn, Influence of surface temperature, ion impact energy, and bulk tungsten content on the sputtering of steels: In situ observations from plasma exposure in PSI-2, Nuclear Materials and Energy 33 (Oct. 2022) 101244, https://doi.org/10.1016/j.nme.2022.101244.
[9] K.R. Yang, et al., Modelling of physical sputtering properties during tungsten fuzz growth under various impact energies on NAGDIS-II, J. Nucl. Mater. 588 (2024) 154783, https://doi.org/10.1016/j.jnucmat.2023.154783.
[10] S. Möller, O. Kachko, M. Rasinski, A. Kreter, C. Linsmeier, In situ investigation of helium fuzz growth on tungsten in relation to ion flux, fluence, surface temperature and ion energy using infrared imaging in PSI-2, Phys. Scr. T170 (Sep. 2017) 014017, https://doi.org/10.1088/1402-4896/aa8a0a.
[11] V. Kh. Alimov, et al., Surface morphology of F82H steel exposed to low-energy D plasma at elevated temperatures, J. Nucl. Mater. 510 (2018) 366–372, https://doi.org/10.1016/j.jnucmat.2018.08.037.
[12] A. Kreter, et al., Linear plasma device PSI-2 for plasma-material interaction studies, Fusion Sci. Technol. 68 (1) (2015) 8–14, https://doi.org/10.13182/FST14-906.
[13] S. Möller, et al., A new high-throughput focused MeV ion-beam analysis setup, Instruments 5 (1) (2021) 1, https://doi.org/10.3390/instruments5010010.
[14] O.V. Ogorodnikova, et al., Surface modification and deuterium retention in reduced-activation steels under low-energy deuterium plasma exposure. Part II: steels pre-damaged with 20 MeV W ions and high heat flux, Nucl. Fusion 57 (3) (2017) 036011, https://doi.org/10.1088/1741-4326/57/3/036011.
[15] Q. Shi, S. Dai, D. Wang, 3D modelling of tungsten fuzz growth under the bombardment of helium plasma, Fusion Eng. Des. 136 (2018) 554–557, https://doi.org/10.1016/j.fusengdes.2018.03.019.
[16] V. Kh. Alimov, et al., Surface modification and sputtering erosion of reduced activation ferritic martensitic steel F82H exposed to low-energy, high flux

deuterium plasma, Nucl. Mater. Energy 7 (2016) 25–32, https://doi.org/10.1016/j.nme.2016.01.001.